Reprinted from APPLIED OPTICS, Vol. 20, page 2861, August 15, 1981

Expanded-beam connector design study

J. C. Baker and D. N. Payne

A theoretical analysis of an expanded-beam connector is presented, and it is shown that considerable scope exists for optimization of the design. A ray-tracing technique is used to quantify the importance of various parameters in determining the insertion loss. The design guidelines are presented in graphical form, and their usefulness is demonstrated in several examples of practical interest.

I. Introduction

A number of demountable-connector designs for use with multimode optical fibers have been reported in recent years.[1–3] These may be classified into two types: (1) those in which the fibers are directly butted together and (2) those which incorporate an optical lensing system[2,3] to project an image of the emitting fiber onto the face of the receiving fiber (expanded-beam connectors). In the case of a butt connector, a lateral alignment tolerance of no greater than 10% of the core radius must be maintained to avoid losses exceeding 0.3 dB.[4] This degree of precision can prove difficult to achieve repeatably, particularly in dirty or hostile environments. The expanded-beam connector, on the other hand, has a potential advantage, since the fiber termination incorporates a lens which serves both to protect the fiber end and to enlarge the emitting area which is presented to the atmosphere. The connector is then more robust and less sensitive to ingress of dust and other forms of contamination. Moreover, it has an insertion loss which is less sensitive to the effect of lateral misalignment of the fiber–lens assemblies, although this is obtained at the expense of an increased sensitivity to the effect of angular misalignment. Fortunately, the latter is relatively easy to avoid mechanically. However, in the expanded-beam connector, the alignment of the fibers to the axes of the lenses must be as accurate as that of the fibers in a butt connector. Whereas this can prove troublesome when using conventional lenses, it is possible to exploit the natural symmetry of a sphere lens to achieve a self-centering action. One of the first designs[5] to utilize the principle is shown in Fig. 1 where the fiber is terminated by a sphere and shell assembly to form one half of a connector. The region between the fiber and sphere is filled with an index-matching material. The fiber is centered with respect to the sphere lens and is precisely positioned at the lens focal point so that the output beam is collimated. The beam is then refocused by a second identical termination (not shown) which houses the receiving fiber.

Despite their obvious attractions, expanded-beam connectors have not seen widespread adoption largely because of their high insertion loss in comparison with that of butt-type connectors. The difference is accounted for by aberrations in the lensing system, which degrade the quality of the image that is presented to the receiving fiber. We have carried out an analysis of a class of expanded-beam connectors with two objectives in mind: first, to estimate the importance of various parameters in determining the insertion loss and, second, to provide a set of criteria for optimization of the design. It is shown that the intuitive results of thin lens theory are in qualitative agreement with our results; thus, for example, the lenses should in general be spaced at twice their focal length to ensure that off-axis rays pass through the connector symmetrically. For an optimum design and a realistic fiber excitation condition we compute that the effect of aberrations on connector loss amount to 0.4 dB for a fiber N.A. of 0.2. This contribution increases to 0.6 dB for a fiber N.A. of 0.3. Thus with careful design sphere–lens connectors can have a loss comparable with that of a butt connector.

II. Ray-Tracing Theory

The model used in the analysis is shown in Fig. 2. Each identical termination is assumed to have a single refracting surface with radius of curvature R, the region between this surface and the fiber having a uniform isotropic refractive index n. This is the configuration,

The authors are with University of Southampton, Electronics Department, Southampton, Hampshire S09 5NH, U. K.

Received 28 January 1981.
0003-6935/81/162861-07$00.50/0.

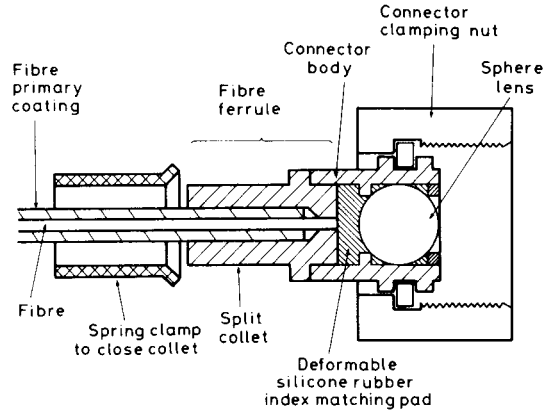

Fig. 1. Exploded view of expanded-beam connector incorporating a sphere lens.

fiber to lens spacing do not in general correspond to the focal length f_g in glass for paraxial rays [$f_g = nR/(n-1)$].

Consider a wave vector $\mathbf{k}_1$ of length n representing a ray originating from fiber 1. The components of $\mathbf{k}_1$ are

$$\mathbf{k}_1 = n(\hat{x}\sin\theta_1\cos\phi_1 + \hat{y}\sin\theta_1\sin\phi_1 + \hat{z}\cos\theta_1), \quad (1)$$

where $\hat{x}, \hat{y}$, and $\hat{z}$ are the unit vectors along the x, y, and z axes, respectively, and θ_1, ϕ_1, and n are the spherical coordinates.

The point at which the ray exits the fiber can be referenced to the center of the radius of curvature of lens 1 as follows:

$$\mathbf{a}_1 = \hat{x}r\cos\phi + \hat{y}r\sin\phi - \hat{z}\left(\frac{R}{n-1} + \Delta f\right), \quad (2)$$

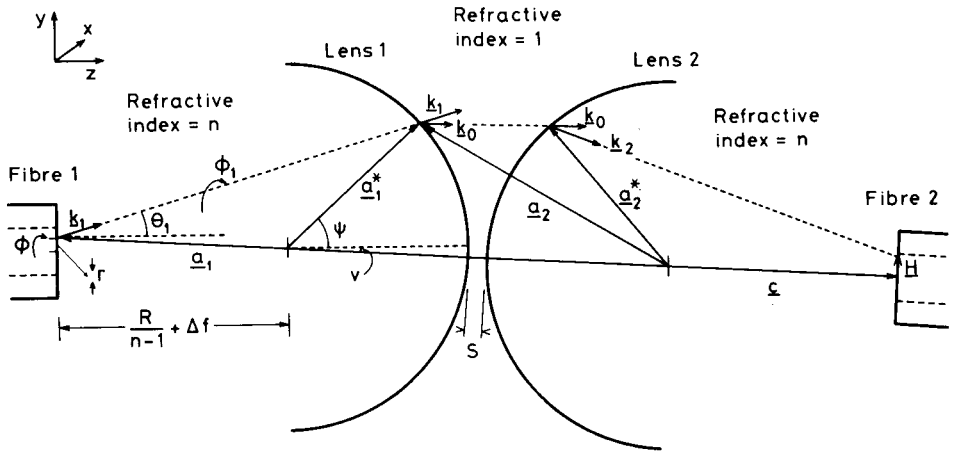

Fig. 2. Schematic diagram of expanded-beam connector showing the vector quantities employed in the analysis. ϕ is the radial angular coordinate of the origin of a ray on the end face of fiber 1. ϕ_1 is the radial angular coordinate of the direction of the ray.

for example, in the design shown in Fig. 1, where the spherical lens is closely index-matched to the fiber. The model is also applicable to connectors incorporating rod lenses[3] which likewise rely on a single refracting surface for collimation. Six parameters were considered, namely, the lens radius of curvature/fiber core radius (R/F), the fiber N.A., the lens refractive index n, the relative tilt and spacing between the lenses (v and s, respectively), and the axial position of the fiber relative to the focal point for paraxial rays (Δf).

The last parameter is relevant because marginal rays, i.e., those rays with a large azimuthal angle θ_1, will be brought to a focus in a region slightly closer to lens 2 than the focal point for paraxial rays, for which $\theta_1 \sim 0$. This is the well-known phenomenon of spherical aberration, which gives rise to a circle of least image confusion. Since marginal rays form the majority of those traced, the circle of least confusion and the optimum

where ϕ is the radial angle in the plane of the fiber end-face (see Fig. 2).

To trace the ray through lens 1 we must find the vector coordinates of the point at which the ray is refracted ($\mathbf{a}_1^*$) and the unit length wave vector after refraction ($\mathbf{k}_0$).[6]

Two scale factors (l_1 and p_1) are introduced:

$$\mathbf{a}_1^* = \mathbf{a}_1 + l_1\mathbf{k}_1; \quad (3)$$

$$\mathbf{k}_0 = \mathbf{k}_1 - p_1\mathbf{a}_1^*; \quad (4)$$

where Eq. (4) is a vector statement of Snell's law. We adopt the convention that the radius of curvature of lens 1 is positive, and that of lens 2 is negative. To solve Eqs. (3) and (4) for l_1 and p_1, respectively, we take the dot product of Eq. (3) by $\mathbf{k}_1$ and Eq. (4) by $\mathbf{a}_1^*$ to obtain

$$n^2 l_1 = \mathbf{a}_1^* \cdot \mathbf{k}_1 - \mathbf{a}_1 \cdot \mathbf{k}_1, \quad (5)$$

$$R^2 p_1 = \mathbf{a}_1^* \cdot \mathbf{k}_1 - \mathbf{a}_1 \cdot \mathbf{k}_0. \tag{6}$$

We now introduce the invariant $\mathbf{J}_1$:

$$\mathbf{J}_1 = \mathbf{a}_1 \times \mathbf{k}_1 = \mathbf{a}_1^* \times \mathbf{k}_1 = \mathbf{a}_1^* \times \mathbf{k}_0, \tag{7}$$

where $\times$ denotes the cross product. The equality of the last two terms is also a vector statement of Snell's law.

By use of the vector identity

$$(\mathbf{a} \times \mathbf{k})^2 = \mathbf{a}^2 \cdot \mathbf{k}^2 - (\mathbf{a} \cdot \mathbf{k})^2, \tag{8}$$

we obtain from Eqs. (5), (6), and (7)

$$l_1 = \frac{1}{n^2}[R\sqrt{n^2 - (J_1/R)^2} - \mathbf{a}_1 \cdot \mathbf{k}_1], \tag{9}$$

$$p_1 = \frac{1}{R}[\sqrt{n^2 - (J_1/R)^2} - \sqrt{1 - (J_1/R)^2}], \tag{10}$$

where the value of J_1^2 is obtained from the first term in Eq. (7). The values of $\mathbf{k}_0$ and $\mathbf{a}_1^*$ are now obtained directly from Eqs. (3) and (4).

The coordinate system is now referred to the center of curvature of lens 2 by means of the transformation

$$\mathbf{a}_2 = \mathbf{a}_1^* - (2R + s)(\hat{y} \sin\upsilon + \hat{z} \cos\upsilon). \tag{11}$$

The procedure of Eqs. (2)–(10) is repeated to find the values of $\mathbf{a}_2^*$ and $\mathbf{k}_2$, where

$$\mathbf{a}_2^* = \mathbf{a}_2 + l_2 \mathbf{k}_0, \tag{12}$$

$$\mathbf{k}_2 = \mathbf{k}_0 + p_2 \mathbf{a}_2^*. \tag{13}$$

For l_2 and p_2 we find

$$l_2 = -R\sqrt{1 - (J_2/R)^2} - \mathbf{k}_0 \cdot \mathbf{a}_2, \tag{14}$$

$$p_2 = -\frac{1}{R}[\sqrt{n^2 - (J_2/R)^2} - \sqrt{1 - (J_2/R)^2}], \tag{15}$$

where

$$\mathbf{J}_2 = \mathbf{a}_2 \times \mathbf{k}_0 = \mathbf{a}_2^* \times \mathbf{k}_2 = \mathbf{a}_2 \times \mathbf{k}_0. \tag{16}$$

To complete the tracing of the ray we must find out whether it is captured (both in position and angle) by fiber 2. A scale factor L is therefore introduced:

$$\mathbf{C} + \mathbf{H} = L\mathbf{k}_2 + \mathbf{a}_2^*, \tag{17}$$

where

$$\mathbf{C} = \hat{y}\left(\frac{R}{n-1} + \Delta f\right)\sin\upsilon + \hat{z}\left(\frac{R}{n-1} + \Delta f\right)\cos\upsilon. \tag{18}$$

Now $\mathbf{C} \cdot \mathbf{H} = 0$ and thus (19)

$$L = \frac{C^2 - \mathbf{a}_2^* \cdot \mathbf{C}}{\mathbf{k}_2 \cdot \mathbf{C}}. \tag{20}$$

The position of the ray is now obtained by calculating $\mathbf{H}$ from Eq. (17), while the corresponding azimuthal angle is the angle between $\mathbf{C}$ and $\mathbf{k}_2$.

We are now in a position to trace through the connector a set of rays representative of a given excitation condition of fiber 1. The loss is computed by counting the fraction which are accepted by fiber 2. It was found necessary to trace 10^4 rays per loss calculation to keep the scatter between estimates to an acceptable level. Note that to isolate the effect of optical aberrations, Fresnel reflection losses have not been included in the present calculations.

In the case where the terminations are tilted ($\upsilon > 0$), the connector no longer possesses an axis of cylindrical symmetry. It was thus necessary to consider carefully how the distribution of rays was to be generated. Care was taken to ensure that the rays launched were randomly distributed in position and angle. If a regular pattern were generated, it would possess an orientation with respect to the tilt plane, and this might bias the result of the loss calculation.

Since the expanded-beam connector has an insertion loss dominated by spherical aberration, the loss will vary according to the angular and spatial distribution of the light presented by the emitting fiber. The greater the proportion of paraxial rays, i.e., lower-order modes, the lower will be the loss. It is thus important to consider the excitation of the emitting fiber, since this will directly influence the computed loss. We have chosen to study a step-index fiber under two excitation conditions: (1) under excited and (2) fully excited. The former should be representative of the majority of fibers met in practice, whereas the latter represents the worst case. The results for these two conditions should thus provide an indication of the range of loss values likely to be found.

III. Partially Excited Fiber

We first consider a fiber excitation condition in which power is predominantly contained in lower-order modes. A number of possible models could be taken to represent the angular and spatial distribution of power likely to be met in practice. For the sake of simplicity we consider here a step-index fiber having a distribution in which rays originate from an equal number of points on each of a series of equispaced concentric circles on the end face. While the spacing of a set of points around a circumference was regular, each set was randomly orientated with respect to its neighbors. Similarly, at a given point the number of rays traced per unit radial angle ϕ_1 at a given azimuthal angle θ_1 was kept constant (i.e., independent of θ_1). Once again, while the spacing of a set of rays having a given θ_1 was regular, each set was orientated randomly with respect to its neighbors.

The problem of optimizing a design in the face of so many interdependent variables is that it is strictly necessary to vary them all continuously until the optimum is found. Obviously this is a very time-consuming approach, and we are thus guided by the predictions of thin-lens theory and consider first the lens spacing s, since we expect to find a single optimum value, equal to twice the lens focal length in air [$f_a = R/(n - 1)$].

At this spacing all rays pass through the optical system symmetrically and thus form an image which faithfully reproduces the distribution of light from the emitting fiber angularly as well as spatially. For all other lens spacings the angular content of the image does not correspond to that of the emitting fiber, and therefore some rays may fall outside the N.A. of the receiving fiber. Thus the optimum value of lens spacing should not be strongly dependent on the other variables.

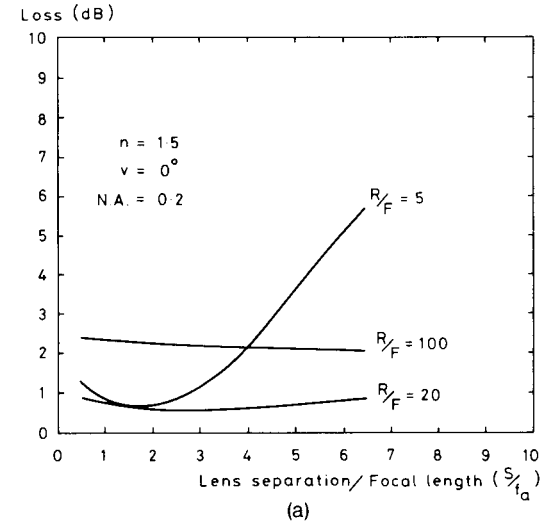

Fig. 3. Loss as a function of (lens separation)/(focal length of lens in air) (s/f_a) in the case of a partially excited fiber. Lenses are untilted ($v = 0$). For each figure a different lens refractive index n is considered: (a) $n = 1.5$; (b) $n = 1.78$; (c) $n = 2.0$. In each case, the curves are drawn for three values of (lens radius of curvature)/(fiber radius) (R/F).

The relationship between loss and lens spacing is plotted in Fig. 3. For the moment we assume that the fibers are placed at the lens focal points, i.e., $\Delta f = 0$. We see that a single optimum does indeed exist at the predicted separation. The effect is small for $R/F \gtrsim 20$, since, for sufficiently large values of R/F, all rays originate from points close to the axis and thus are highly collimated. Henceforth, for this launch condition we present our results with the lenses spaced at $2f_a$. In addition we see that the loss curve for $n = 1.5$ and $R/F = 100$ is relatively high. To explain this, we note that spherical aberration increases with increasing beam expansion h. In our particular case, the fibers are always placed at the focal length f_g so that

$$h \simeq 1 + \left(\frac{R}{F}\right)\left[\frac{1}{n-1} + \cos\psi\right]\tan\theta_M, \tag{21}$$

where $\theta_M = asn(\text{N.A.}/n)$ and is related to the angle ψ (Fig. 1). While an examination of this equation reveals that h and hence the effect of spherical aberration increase with decreasing n, it is perhaps better to visualize the constraints at work: as we decrease n, both the focal length $[f_g = nR/(n-1)]$ and the half angle of the cone of rays emitted by fiber 1 $[= asn(\text{N.A.}/n)]$ increase; hence h and the effect of spherical aberration also increase. Furthermore, a large value of R/F means a relatively small cross section for capture of rays by fiber 2, so that a given spherical aberration has a greater effect on insertion loss.

Having decided upon the optimum lens separation, the relationship between loss and (R/F) is plotted as a function of tilt v in Fig. 4. The upper horizontal scale gives the approximate beam expansion obtained from Eq. (21). As we should expect from the foregoing discussion, for a given value of R/F a high refractive-index lens is not so effective in expanding the output beam. The curves confirm that the loss is much more susceptible to tilt than in the case of butt-type connectors. The effect of optimally spacing the lenses can also be seen, in that quite small values of R/F ($\sim$5) can be tolerated without incurring a serious loss penalty.

We now turn to the question of mitigating the effect of spherical aberration in the case where high N.A. fibers are specified, and therefore the image aberrations are more troublesome. As outlined earlier, we might expect an improvement in the loss by moving the fibers slightly closer to the lenses, i.e., toward the circle of least confusion, and this prediction is confirmed in Fig. 5 where the relationship between loss and Δf is plotted for $R/F = 20$. We see that the minima for various values of N.A. and sphere index are within 0.2 dB of each other, so that a large degree of compensation is possible. In particular, it is possible to reduce the losses from 1.6 to 0.6 dB for the $n = 1.5$, N.A. = 0.3 case.

Examples: Suppose we wish to terminate a 100-μm core diam, N.A. = 0.2, step-index fiber using a spherical glass ($n = 1.5$) ball as a lens, the space between the ball and the fiber being filled with an index-matching material. As a further constraint, suppose the ball is to fit into a standard connector shell so that its diameter is fixed at, say, 2 mm. Then $R/F = 20$, and we see from Fig. 3(a) that, while a small benefit is to be obtained by

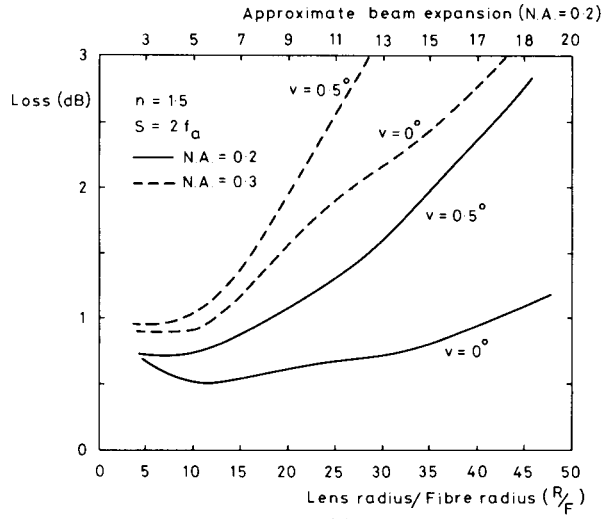

(a)

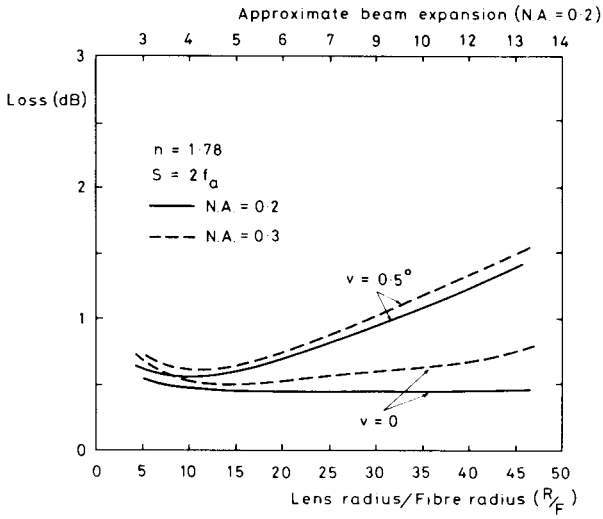

(b)

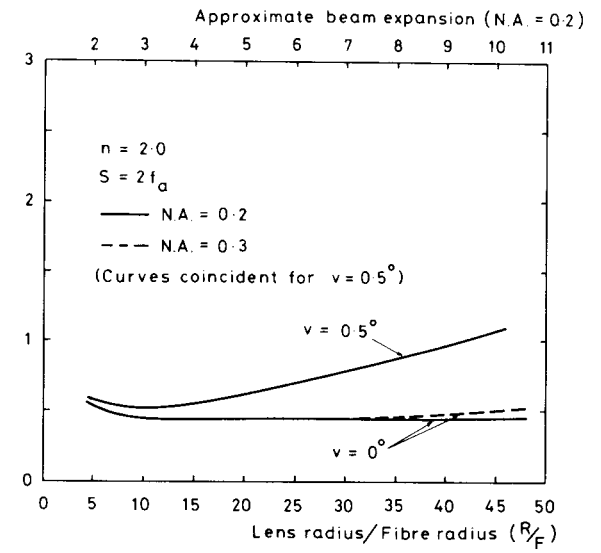

(c)

Fig. 4. Loss as a function of (lens radius of curvature)/(fiber radius) (R/F) in the case of a partially excited fiber. Lenses are optimally spaced ($s = 2f_a$). For each figure a different lens refractive index n is considered: (a) $n = 1.5$; (b) $n = 1.78$; (c) $n = 2.0$. In each case, the curves are drawn for various values of tilt v and N.A.

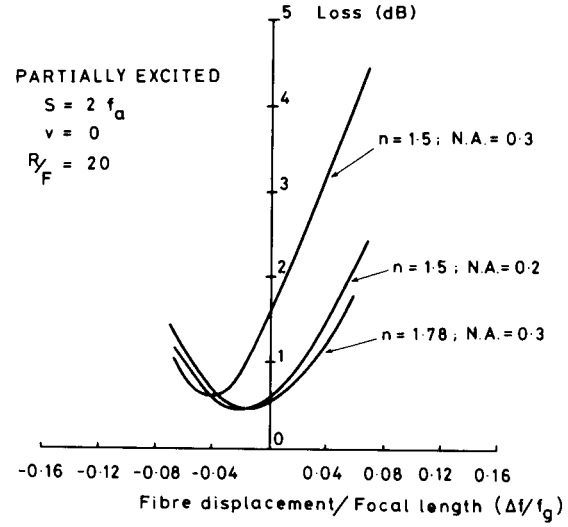

Fig. 5. Loss as a function of (fiber displacement from paraxial focus)/(paraxial focal length in glass) $(\Delta f/f_g)$ in the case of a partially excited fiber. Lenses are untilted ($v = 0$) and optimally spaced ($s = 2f_a$). (Lens radius of curvature)/(fiber radius) $(R/F) = 20$, and the curves are drawn for various values of N.A. and lens refractive index n.

spacing the balls at $2f_a$, this parameter is not critical. A beam expansion of ~9 times will be obtained, and the loss is therefore determined by the tilt tolerance; <1 dB might be expected if this tolerance could be kept below 0.5°. By choosing $\Delta f = -180$ μm this might be reduced to 0.8 dB. To this figure must be added the Fresnel reflection loss for two surfaces, unless antireflection coatings are used.

By way of comparison, suppose we now wish to simply protect the end of a 400 μm core diam step-index fiber having an N.A. of 0.3. With such a large core size, there is little point in expanding the beam by having a large value of R/F, since this will increase the susceptibility of the insertion loss to tilt. Thus we take the same value of lens curvature as in the previous example. In this case we might choose sapphire ($n \sim 1.78$) as the lens material because of its hardness. $R/F = 5$, and we infer from Fig. 3(b) that a definite advantage is obtained by spacing the lenses by $2f_a$. Figure 4(b) indicates that the beam expansion is small (~3 times), and the dependence of insertion loss upon tilt is correspondingly relaxed; a tilt of 0.5° can be tolerated without significant increase in loss. Furthermore, we can infer from Fig. 5 that there would be little benefit in placing the fiber at other than the focus for paraxial rays (i.e., $\Delta f = 0$).

IV. Fully Excited Fiber

We now turn to consider the fully excited step-index fiber condition which is characterized by the requirement that the number of rays emitted per unit area per unit solid angle is constant. As before, ray coordinates were randomized by a procedure similar to that applied in the case of the partially excited launch. This case is little more complicated because there is a relatively large number of marginal rays, so the effect of spherical

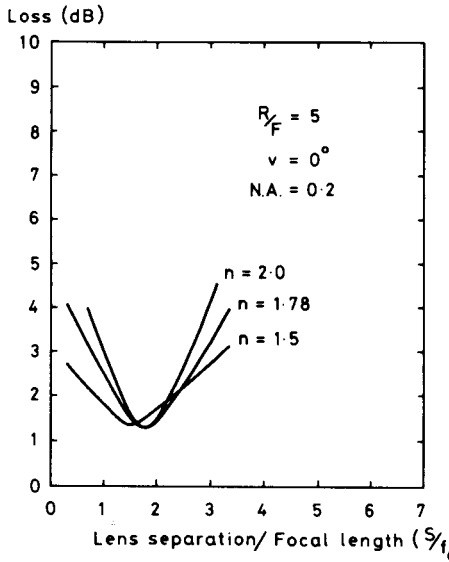

Fig. 6. Loss as a function of lens separation)/(focal length of lens in air) (s/f_a) in the case of a fully excited fiber. Lenses are untilted (v = 0), and N.A. = 0.2. (Lens radius of curvature)/(fiber radius) (R/F) = 5, and the curves are drawn for various values of lens refractive index n.

case of partial excitation; the differences are consistent with the effect of launching a larger proportion of marginal rays. Thus the minimum loss is higher, and it is found that for an N.A. of 0.2 the contribution made by aberrations is close to 1 dB, increasing to ~1.5 dB for an N.A. of 0.3.

V. Conclusions

We have carried out a theoretical design study of an expanded-beam connector to quantify the importance of several parameters and obtain a set of design criteria. By careful choice of the design parameters we find that for a step-index fiber having an N.A. of 0.2 the contribution of spherical aberration to the total loss falls in the 0.4–1.1-dB range for partially and fully excited launch conditions, respectively. The range becomes 0.6–1.65 dB upon increasing the fiber N.A. to 0.3. Among the important design parameters to emerge are:

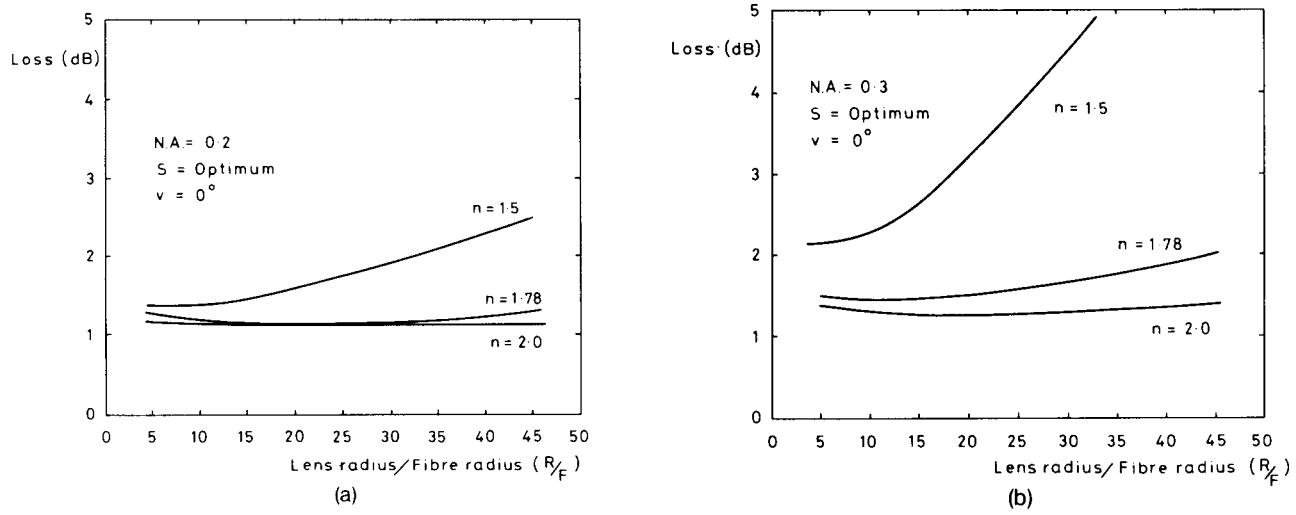

Fig. 7. Loss as a function of (lens radius of curvature)/(fiber radius) (R/F) in the case of a fully excited fiber. Lenses are untilted (v = 0) and are optimally spaced. For each figure a different N.A. is considered: (a) N.A. = 0.2; (b) N.A. = 0.3. In each case, the curves are drawn for various values of the lens refractive index n.

aberration is greater. In Fig. 6 the relationship between loss and lens separation (s/f_a) is plotted, and we find that a lens separation of $2f_a$ is not so universally appropriate, a value of $1.5\,f_a$ being a better choice for n = 1.5. We see from Figs. 7 that the dependence of loss on R/F is more pronounced, particularly for n = 1.5, and we would therefore expect the effect of varying Δf to be more important. This is confirmed in Fig. 8 where we find a significant benefit is obtained even for n = 1.78.

In general, the curves obtained for the fully excited fiber are qualitatively similar to those obtained in the

(1) Lens spacing. This parameter is effective in bringing off-axis rays to a focus in the receiving fiber image plane and should in general be twice the lens focal length in air.

(2) Displacement of the fiber relative to the focus for paraxial rays. Varying this parameter is effective in mitigating the effect of spherical aberration and ensures that the receiving fiber captures a larger proportion of the marginal rays. The optimum value is a strong function of N.A. and amounts to a displacement of as much as 5% of the lens focal length in a direction toward the lens.

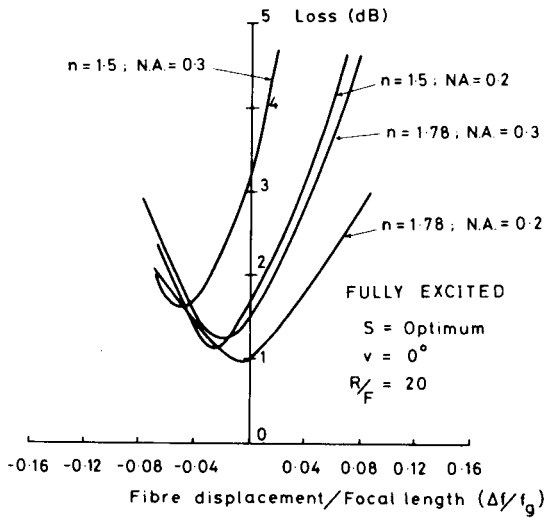

Fig. 8. Loss as a function of (fiber displacement)/(paraxial focal length in glass) ($\Delta f/f_g$) in the case of a fully excited fiber. Lenses are untilted ($v = 0$) and are optimally spaced. The (lens radius of curvature)/(fiber radius) (R/F) = 20 and the curves are drawn for various values of lens refractive index n and N.A.

(3) Lens radius of curvature/fiber radius. This parameter determines the beam expansion and consequently the susceptibility of the loss to angular misalignment. The exact choice depends upon the characteristics of the fiber and the trade-off that exists between the angular and lateral misalignment tolerance.

We believe that the conclusions of this design study establish the expanded-beam connector as an attractive alternative to the butt-connector, particularly in hostile environments or where a long active service life is envisaged. Furthermore, if the added complication of a lens doublet can be tolerated it is possible to envisage a considerable reduction in spherical aberrations and, consequently, lower losses.

The authors wish to express their thanks to M. J. Adams and A. Ankiewicz for useful discussions. Grateful acknowledgment is made to the U.K. Ministry of Defence for funding the work and the Pirelli General Cable Co. for the award of a research fellowship.

References

1. C. Kao and G. Bickel, "Fiber Connectors, Splices and Couplers," in *Fiber Optics* B. Bendow and S. S. Mitra, Eds. (Plenum, New York, 1979).
2. A. Nicia, Electron. Lett. **14**, 511 (1978).
3. J. C. North and J. H. Stewart, "A Rod Lens Connector for Optical Fibres," in *Technical Digest, Fifth ECOC, Amsterdam, 1979*, Sec. 9.4.
4. M. J. Adams, D. N. Payne, and F. M. E. Sladen, Appl. Phys. Lett. **28**, 524 (1976).
5. Reproduced with permission from J. P. Dakin, M. G. Holliday, and R. J. Hall, Plessey Co. Ltd, Southleigh, Hampshire, England.
6. M. Herzberger, *Modern Geometrical Optics* (Interscience, New York, 1958).